Progress In Electromagnetics Research B, Vol. 16, 189–207, 2009

ANALYTICAL COMPUTATION OF THE ELECTROMAGNETIC FIELD PRODUCED BY AN OPTICAL FIBER HELIX

I. Chremmos

Microwave and Fiber Optics Laboratory
School of Electrical and Computer Engineering
National Technical University of Athens
9 Iroon Polytechniou Str., Zografos 15780, Athens, Greece

Abstract—A completely analytical computation of the electromagnetic field produced by an optical fiber helix is presented for the first time. The analysis utilizes the transformation of radially traveling cylindrical waves between two skew cylindrical coordinates systems, that has been previously derived by the author, in order to express the waves radiated by each infinitesimal part of the helix in terms of cylindrical waves around the helix axis and be able to integrate the contributions analytically. Under certain realistic geometrical assumptions, an unperturbed propagation of a single fiber mode is assumed to account for the infinite fiber length, leading to elegant final series expressions in terms of mixed angular-axial Hartree space harmonics, which show clearly the effect of the helical geometry on the field distribution. Analytical formulas are obtained for the field inside and outside the helix cylinder and an interesting two-term decomposition of the outward radiated field is concluded.

1. INTRODUCTION

In a previous work [1], we derived the transformation of radially traveling cylindrical waves, namely waves with a Hankel-function radial dependence of complex argument, between two cylindrical coordinate systems with skew (non-parallel) axes. This is a 3D generalization of the classic 2D Graf's addition theorem for Hankel functions [2] that has been extensively used over the past 100 years to express cylindrical waves between displaced polar coordinate systems. The analytical

Corresponding author: I. Chremmos (jochremm@central.ntua.gr).

proof of the new theorem derived in [1] was based on the fundamental integral representation of Hankel function on the complex plane and, subsequently, on appropriate deformation of the integration contour and change of variables to finally obtain a Fourier transform of the cylindrical wave around the new system with the skew axis. So far, we have exploited this formula in its arguably most apparent application, which is the evanescent-field coupling between two non-parallel optical fibers, i.e., two fibers with skew axes. With the advent of miniaturized optical fiber components [4], the fundamental configuration of 3D inter-fiber coupling is expected to be present in a variety of optical experiments, thus proving the utility of the above transformation.

In this work we address theoretically a perhaps not so obvious problem in which a 3D transformation of cylindrical waves is also required: The computation of the electromagnetic field produced by a coiled optical fiber, which is formulated using the ideal geometrical structure of a helix. Structures of coiled optical fibers, especially of sub-wavelength diameter, are currently attracting interest as sensitive optical microresonators [5, 6]. The evanescent field of these ultra-thin optical wires is greatly enhanced, causing the periodic interaction between the helix turns and consequently a resonant transmission spectrum. These phenomena have been successfully predicted using the coupled-mode theory formalism [7]. Yet from a different, electromagnetic point of view, it would be of theoretical and practical interest to model the complex distribution of the evanescent field of these coils. To the best of our knowledge, the present paper is the first work addressing this issue and, moreover, attempting an analytical approach by virtue of the previously obtained analytical tool.

To understand the connection of the present problem with the transformation of cylindrical waves between skew axes, note that, according to Green's theorem, the electric field produced by a fiber (or any optical waveguide) anywhere in space is the result of integration of the inner product $\underline{\mathbf{G}}_0(\mathbf{r}, \mathbf{r}') \cdot \mathbf{E}(\mathbf{r}')$ over the entire volume of the fiber, where $\underline{\mathbf{G}}_0$ is the free-space dyadic Green's function and $\mathbf{E}$ is the electric field inside the fiber. In this integral, each infinitesimal part of the fiber with length ds contributes a field $d\mathbf{E}$ that has a cylindrical-eigenwaves expansion with respect to the local system whose z-axis is tangent to the helix at the current point of integration. The summation (integration) of these contributions from all parts of the fiber is impossible to perform analytically because the cylindrical waves emanated from different parts of the fiber refer to different coordinate systems. If however the theorem of [1] is used, each contribution $d\mathbf{E}$ obtains an expression in terms of cylindrical waves referring to the central axis (axis of the helix), thus enabling the integration to

be performed. Furthermore, due to the defining angle property of a helix, each infinitesimal part ds of the fiber is at the same angle with the central axis, which means that the transformation matrix appears conveniently as a common factor of all contributions $d\mathbf{E}$.

2. ANALYSIS

In this paper, we focus on the external electromagnetic field produced by an optical fiber coiled in a helix pattern, as shown in Fig. 1. According to Green's theorem (second Green's identity), the electric field anywhere in the structure in the absence of external sources, is given by the familiar integral which is carried out over the entire fiber volume [8]

$$\mathbf{E}(\mathbf{r}) = \left(k_f^2 - k_0^2\right) \iiint\limits_{fiber} \underline{\mathbf{G}}_0 \left(\mathbf{r}, \mathbf{r}'\right) \cdot \mathbf{E}(\mathbf{r}') dV' \tag{1}$$

where $\underline{\mathbf{G}}_0$ is the free-space dyadic Green's function and $k_f = \omega n_f / c$, $k_0 = \omega / c$ are, respectively, the wave numbers of the fiber material and free-space, n_f is the fiber refractive index, ω the angular frequency and c the speed of light in vacuum. The problem is nonmagnetic, i.e., a constant magnetic permeability μ_0 is present everywhere. Harmonic time dependence $\exp(j\omega t)$ is assumed and suppressed throughout the analysis.

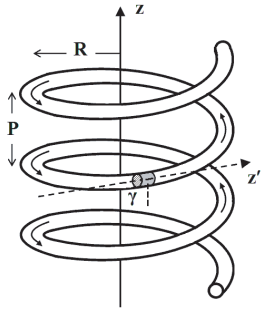

Figure 1. Optical fiber helix with radius R and pitch P. The central z-axis (axis of the helix) and the local z'-axis are skew at an angle γ which is constant as the point of integration runs along the helix. The infinitesimal cylindrical volume dV' that is used in the integration is shown. The arrows indicate the direction of light propagation.

Equation (1) is valid for observation points $\mathbf{r}$ lying inside or outside the volume of the fiber. In the first case, (1) becomes a homogeneous

Fredholm integral equation of the second kind for the electric field inside the fiber. Its solution $\mathbf{E}(\mathbf{r})$ can be subsequently substituted into (1) to provide the field in the exterior of the fiber. However, the solution of the electric field integral equation for a fiber helix is extremely difficult to obtain, even using a numerical technique such as an entire- or sub-domain method of moments. Instead, we will here exploit some useful simplifying assumptions that will maximize our ability to treat such a complex problem analytically and, furthermore, allow us to investigate the utility of the generalized addition theorem of [1]. This is of course a common practice in electromagnetics, since the analytical solutions obtained after some realistic simplifying assumptions have been made are often indicative of phenomena and conclusions that are difficult, if not impossible, to obtain with "blind" numerical modelling.

The basic hypothesis in our problem will be that the field inside the fiber helix is the same with that of a straight fiber. This is a reasonable assumption for helices with geometric parameters that satisfy certain conditions: Firstly, the helix radius (R) must be sufficiently large so that the bend-induced loss and profile perturbation of the guided fiber mode is small. Secondly, the helix pitch (P) must also be sufficiently large so that the coupling between the turns is weak enough and consequently the effect on the mode in the core is small. The latter is a necessary condition for the application of coupled-mode theory analysis too [7]. Thirdly, the ratio P/R of the helix pitch to the helix radius should be sufficiently small so that the coupling between different polarization states of the fiber mode is negligible. In this case, an adiabatic approximation of parallel transport of a bound fiber mode with unperturbed profile along the helix is valid. A thorough discussion on the above conditions can be found in [7] and will not concern us further.

2.1. Cylindrical Vector Wave Functions and Coordinate Transformations

Before proceeding to the analysis, we will quote the definitions of the cylindrical vector wave functions $\mathbf{M}$, $\mathbf{N}$ and the corresponding formulas that transform these waves between different coordinate systems. The latter will be useful for changing coordinate systems while performing the integration (1) along the fiber helix. To this end, consider the cylindrical coordinates (ρ, φ, z) in a medium with wave number k_m. The solenoidal (divergenceless) solutions of the homogeneous vector Helmholtz equation $(\nabla^2 + k_0^2)\mathbf{E} = 0$ are the cylindrical TE_z and TM_z

vector wave functions defined respectively by [9]

$$\begin{aligned}\mathbf{M}_{n,k}^{(i)}(\mathbf{r},k_m) &= \nabla\times\left[\hat{\mathbf{z}}C_n^{(i)}(a_m\rho)e^{j(n\varphi+kz)}\right]\\ \mathbf{N}_{n,k}^{(i)}(\mathbf{r},k_m) &= \frac{1}{k_m}\nabla\times\mathbf{M}_{n,k}^{(i)}(\mathbf{r},k_m)\end{aligned} \tag{2}$$

where $a_m(k)=\sqrt{k_m^2-k^2}$, n is an integer, and the function of the radial dependence can be either $C^1\equiv J$, i.e., Bessel function, or $C^{(2)}\equiv H^{(2)}$, i.e., Hankel function of the 2nd kind. When waves extending to infinity are concerned ($\rho\to+\infty$) the square root defining $a_m(k)$ is chosen with $\mathrm{Re}(a_m)>0$ and $\mathrm{Im}(a_m)<0$, so that the radiation condition is satisfied and the wave amplitude stays finite. After performing the curl operations in (2) the **M**, **N** waves are written explicitly

$$\begin{aligned}\mathbf{M}_{n,k}^{(i)}(\mathbf{r},k_m) &= \left[\hat{\boldsymbol{\rho}}\frac{jn}{\rho}C_n^{(i)}(a_m\rho)-\hat{\boldsymbol{\varphi}}\frac{\partial C_n^{(i)}(a_m\rho)}{\partial\rho}\right]e^{j(n\varphi+kz)}\\ \mathbf{N}_{n,k}^{(i)}(\mathbf{r},k_m) &= \frac{1}{k_1}\left[\hat{\boldsymbol{\rho}}\,jk\frac{\partial C_n^{(i)}(a_m\rho)}{\partial\rho}-\hat{\boldsymbol{\varphi}}\,\frac{nk}{\rho}C_n^{(i)}(a_m\rho)\right.\\ &\quad\left.+\hat{\mathbf{z}}a_m^2C_n^{(i)}(a_m\rho)\right]e^{j(n\varphi+kz)}\end{aligned} \tag{3}$$

The two simplest transformations of vector wave functions **M**, **N** are those applying for a translation of the coordinate system along the z-axis or for a rotation around the z-axis, which are shown respectively

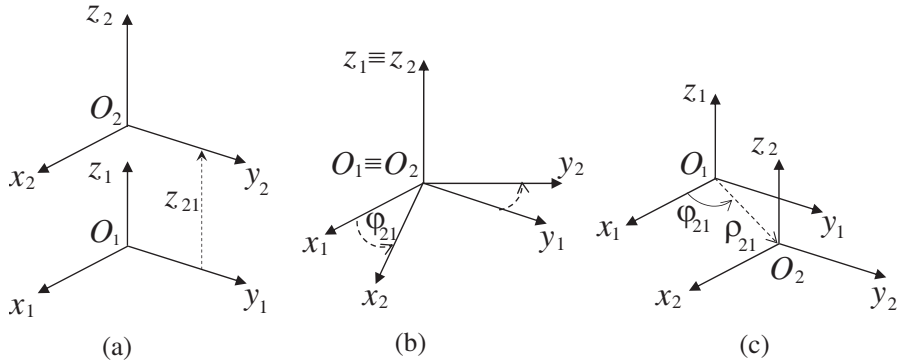

Figure 2. Different system transformations**:** (a) Translation along the z-direction. (b) Rotation around the z-axis. (c) Parallel z-axis translation.

in Figs. 2(a) and 2(b). In both cases the wave functions of the two systems obviously differ only by a phase factor, obtained by the offset in the axial direction in the first case

$$\begin{pmatrix} \mathbf{M}_{n,k}^{(i)}(\mathbf{r}_1, k_m) \\ \mathbf{N}_{n,k}^{(i)}(\mathbf{r}_1, k_m) \end{pmatrix} = \begin{pmatrix} \mathbf{M}_{n,k}^{(i)}(\mathbf{r}_2, k_m) \\ \mathbf{N}_{n,k}^{(i)}(\mathbf{r}_2, k_m) \end{pmatrix} \times e^{jkz_{21}} \tag{4}$$

or in the angular direction in the second case

$$\begin{pmatrix} \mathbf{M}_{n,k}^{(i)}(\mathbf{r}_1, k_m) \\ \mathbf{N}_{n,k}^{(i)}(\mathbf{r}_1, k_m) \end{pmatrix} = \begin{pmatrix} \mathbf{M}_{n,k}^{(i)}(\mathbf{r}_2, k_m) \\ \mathbf{N}_{n,k}^{(i)}(\mathbf{r}_2, k_m) \end{pmatrix} \times e^{jn\varphi_{21}} \tag{5}$$

where $\mathbf{r}_1$, $\mathbf{r}_2$ are the position vectors in systems (1), (2), respectively, z_{21} is the z-coordinate of the origin of system (2) observed in system (1) and φ_{21} is the angle of rotation from system (1) to system (2).

The problem of transforming vector waves $\mathbf{M}$, $\mathbf{N}$ becomes more complicated under a parallel translation of the z-axis, which is shown in Fig. 2(c). This is where Graf's addition theorem applies [2]. The theorem refers to scalar cylindrical wave functions. However, since the two systems have identical $\hat{\mathbf{z}}$ unit vectors, it is straightforward to extend it to vector wave functions by multiplying both sides of the scalar addition theorem with $\hat{\mathbf{z}}$ and applying the curl operator [1]. Here we quote only the case of transforming $\mathbf{M}$, $\mathbf{N}$ waves with Hankel function radial dependence in system (1), which is written

$$\begin{bmatrix} \mathbf{M}_{n,k}^{(2)}(\mathbf{r}_2, k_m) \\ \mathbf{N}_{n,k}^{(2)}(\mathbf{r}_2, k_m) \end{bmatrix} = \sum_{q=-\infty}^{+\infty} H_{q-n}^{(2)}(a_m\rho_{21}) e^{-j(q-n)\varphi_{21}} \begin{bmatrix} \mathbf{M}_{q,k}^{(1)}(\mathbf{r}_1, k_m) \\ \mathbf{N}_{q,k}^{(1)}(\mathbf{r}_1, k_m) \end{bmatrix} \tag{6}$$

which holds for $\rho_1 < \rho_{21}$, where ρ_{21} is the polar distance between the origins of the two systems and φ_{21} is the polar angle of the origin of system (2) observed in system (1). A similar formula applies for waves with a Bessel-function radial dependence, by replacing $H_{q-n}^{(2)}(a_m\rho_{21})$ with $J_{q-n}(a_m\rho_{21})$.

The system transformations of Fig. 2 cover all cases of two coordinate systems with parallel z-axes. The corresponding transformations are simple because the TE_z, TM_z waves stay uncoupled, in the sense that a TE_z wave ($\mathbf{M}$) of the first system is expressed in terms of only TE_z waves in the second system and similarly for the TM_z waves ($\mathbf{N}$). Furthermore, the wave number k in the z-direction is common for both systems. The considerably more complicated case of systems with nonparallel (skew) z-axes is shown in Fig. 3, assuming without loss of generality the invariance of the

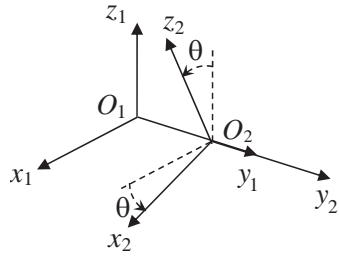

Figure 3. Systems with skew x- and z-axes obtained after a translation along the y-direction by $(O_1O_2) = d$ and a rotation around the y-axis by θ.

y-direction. The corresponding transformations of scalar and vector wave functions were derived in [1]. Here we quote only the version for vector waves

$$\begin{pmatrix} \mathbf{M}^{(2)}_{n,k}(\mathbf{r}_1, k_m) \\ \mathbf{N}^{(2)}_{n,k}(\mathbf{r}_1, k_m) \end{pmatrix} = \int_{-\infty}^{+\infty} dk' \sum_{q=-\infty}^{+\infty} \mathbf{T}^{\theta,d}(q, k'; n, k) \cdot \begin{pmatrix} \mathbf{M}^{(1)}_{q,k'}(\mathbf{r}_2, k_m) \\ \mathbf{N}^{(1)}_{q,k'}(\mathbf{r}_2, k_m) \end{pmatrix} \quad (7)$$

where $\mathbf{T}$ is a symmetric transformation matrix given by

$$\begin{aligned} &\mathbf{T}^{\theta,d}(q,\ k'; n, k) \equiv \begin{bmatrix} \sigma & \tau \\ \tau & \sigma \end{bmatrix} \\ &\begin{pmatrix} \sigma \\ \tau \end{pmatrix} = -j^q \frac{e^{j(k'_y d + n\tau - qw)}}{\pi k'_y} \cdot \begin{pmatrix} \cot\theta + k' \cos w / a'_0 \\ j k_m \sin w / a'_0 \end{pmatrix} \end{aligned} \quad (8)$$

where d and θ are, respectively, the displacement and rotation of the new system (see Fig. 3). Also the following definitions have been made

$$\begin{aligned} a_0 &= \sqrt{k_m^2 - k^2}, \quad (\mathrm{Re}(a_0) > 0,\ \mathrm{Im}(a_0) < 0) \\ a'_0 &= \sqrt{k_m^2 - (k')^2}, \\ k'_x &= \frac{k' \cos\theta - k}{\sin\theta},\ k'_y = \sqrt{(a'_0)^2 - k'^2_x},\ \left(\mathrm{Re}(k'_y) < 0,\ \mathrm{Im}(k'_y) > 0\right) \\ \cos w &= \frac{k'_x}{a'_0},\ \sin w = \frac{k'_y}{a'_0},\ \sin\tau = \frac{k\cos\theta - k'}{a_0 \sin\theta},\ \cos\tau = \frac{k'_y}{a_0}. \end{aligned} \quad (9)$$

The sign of square root a'_0 can be chosen arbitrarily, since this is an argument of standing cylindrical waves (Bessel function) in the new system.

Note from (7) that, contrary to the case of parallel z-axes, both $\mathbf{M}$ and $\mathbf{N}$ waves are required to express a $\mathbf{M}$ or $\mathbf{N}$ wave in the new system and also that an inverse-Fourier transform integral over all wave numbers k' along the z_2-axis is required to express a wave with z_1-dependence $\exp(jkz_1)$.

2.2. Properties of a Helix

Let us now remind some basic properties of a helix. A helix is described by the parametric equations

$$x(\varphi) = R\cos\varphi, \quad y(\varphi) = R\sin\varphi, \quad z(\varphi) = \frac{P\varphi}{2\pi} \tag{10}$$

where the real parameter $\varphi \in (-\infty, +\infty)$ is the polar angle following a point running along the helix, R is the radius and P the pitch (or step) of the helix, i.e., the elevation after a full turn. The tangential unit vector of the helix is $\hat{\mathbf{t}} = \hat{\boldsymbol{\varphi}}\sin\gamma + \hat{\mathbf{z}}\cos\gamma$ where γ is the constant angle of elevation (see Fig. 1), given by $\gamma = \tan^{-1}(2\pi R/P)$. The length of an elementary piece of the helical line for an infinitesimal parameter increment $d\varphi$ is $dS = Rd\varphi/\sin\gamma$. Integrating dS and assuming $S(0) = 0$ yields the length of the helix at a given value of the parameter φ as $S(\varphi) = R\varphi/\sin\gamma$. Finally, the length of a helix turn is $L = S(2\pi) = \sqrt{(2\pi R)^2 + P^2}$.

2.3. Field Computation

Starting with the integral representation (1) and based on the arguments that followed, we turn to the analytical computation of the field produced in the surrounding medium (k_0) of the fiber helix. The analysis uses three different coordinate systems — a fixed and two moving ones — which are shown in Fig. 4:

(1) System (x_0, y_0, z_0) is fixed with the z_0-axis being the axis of the helix. The corresponding cylindrical coordinates (ρ_0, φ_0, z_0) are defined through $x_0 = \rho_0\cos\varphi_0$, $y_0 = \rho_0\sin\varphi_0$. Our aim is essentially to express the field in this global coordinate system.

(2) System (x_h, y_h, z_h) has its origin $x_h = y_h = z_h = 0$ on the fiber axis and moves along the helix as the integration of (1) is performed along the entire fiber length. Its orientation is constantly adjusting so that the unit vector $\hat{\mathbf{z}}_h$ stays tangential to the helical path and the positive semi-axis y_h intersects the axis of the helix. The corresponding cylindrical coordinates (ρ_h, φ_h, z_h) are defined through $x_h = \rho_h\cos\varphi_h$, $y_h = \rho_h\sin\varphi_h$.

(3) System (x_a, y_a, z_a) has as z_a-axis the axis of the helix. It is rotating around this axis and is being elevated as the integration of (1) is performed over the fiber, in such a way that the negative semi-axis y_a passes through the origin of system (2) ($x_h = y_h = z_h = 0$). Obviously, the y-unit vectors of the two moving systems are identical, i.e., $\hat{\mathbf{y}}_h = \hat{\mathbf{y}}_a$ while the x- and z- axes are skew at an angle defined by $\hat{\mathbf{x}}_h \cdot \hat{\mathbf{x}}_a = \hat{\mathbf{z}}_h \cdot \hat{\mathbf{z}}_a = \cos\gamma$. The corresponding cylindrical coordinates (ρ_a, φ_a, z_a) are defined through $x_a = \rho_a \cos\varphi_a$, $y_a = \rho_a \sin\varphi_a$.

We now consider the integral of (1) over an elementary cylindrical slice of the fiber with infinitesimal length dS and volume $dV = \pi\alpha^2 dS$,

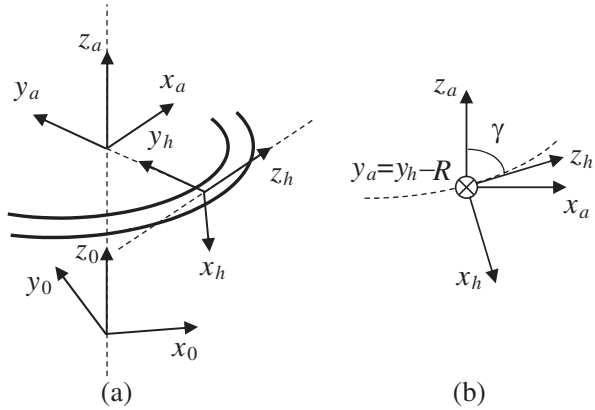

Figure 4. (a) The three coordinate systems used to perform the integration (1). (b) Side view of the two moving systems (x_h, y_h, z_h) and (x_a, y_a, z_a).

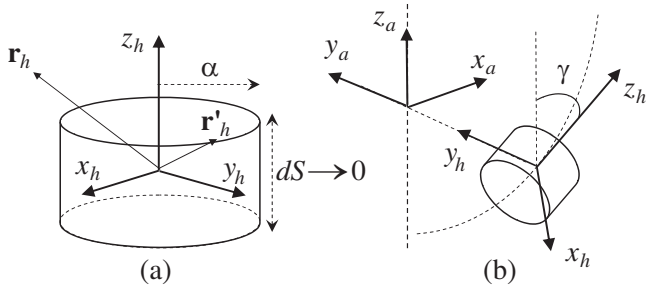

Figure 5. (a) Elementary slice of the fiber for performing the integration (1) and the local system of coordinates (x_h, y_h, z_h). (b) Orientation of the slice in space.

α being the radius of the fiber. In the local system of coordinates (x_h, y_h, z_h), the contribution $d\mathbf{E}$ is written

$$d\mathbf{E}(\mathbf{r}_h) = (k_f^2 - k_0^2) dS \int_0^{\alpha} \rho'_h d\rho'_h \int_0^{2\pi} d\varphi'_h \underline{\mathbf{G}}_0(\mathbf{r}_h, \mathbf{r}'_h) \cdot \mathbf{E}(\mathbf{r}'_h) \qquad (11)$$

The elementary volume and the corresponding local coordinate system are shown in Fig. 5(a). It is important to note that $dS \to 0$ means that the coordinate z'_h can be set constant inside the integral (11) and equal to zero, i.e., $z'_h = 0$. Since we are interested in points $\mathbf{r}_h$ in free-space, we have $\rho'_h \leq \alpha < \rho_h$, a condition that validates an eigenfunction expansion of the free-space dyadic Green's function in terms of radiating waves (Hankel function radial dependence) for point vector $\mathbf{r}_h$ and standing waves (Bessel function radial dependence) for point vector $\mathbf{r}'_h$ [8, 9]. Explicitly

$$\underline{\mathbf{G}}_0(\mathbf{r}_h, \mathbf{r}'_h) = -\frac{j}{8\pi} \times \sum_{n=-\infty}^{+\infty} \int_{-\infty}^{+\infty} dk \frac{(-1)^n}{a_0^2(k)} \left[\mathbf{M}^{(2)}_{n,k}(\mathbf{r}_h, k_0) \quad \mathbf{N}^{(2)}_{n,k}(\mathbf{r}_h, k_0)\right] \begin{bmatrix} \mathbf{M}^{(1)}_{-n,-k}(\mathbf{r}'_h, k_0) \\ \mathbf{N}^{(1)}_{-n,-k}(\mathbf{r}'_h, k_0) \end{bmatrix} \qquad (12)$$

where a grouping of wave functions $\mathbf{M}$, $\mathbf{N}$ as elements of generalized vectors has been used in order to achieve a compact algebraic notation.

Under the conditions that were stated previously, the field inside the fiber has the form of a bound fiber mode propagating along the helical optical path with propagation constant β ($k_0 < \beta < k_f$), i.e., having a dependence $\exp(-j\beta S)$, where S is the helix length at the current point with respect to an arbitrary starting point on the helix (see Section 2.1). Referring to the local coordinate system (x_h, y_h, z_h), the field for $\rho'_h \leq \alpha$ will therefore be

$$\mathrm{E}(\mathbf{r}'_h) = e^{-j\beta S} \left[\mathbf{M}^{(1)}_{m_0,-\beta}(\mathbf{r}'_h, k_f) + \chi \mathbf{N}^{(1)}_{m_0,-\beta}(\mathbf{r}'_h, k_f)\right] \qquad (13)$$

where m_0 is the angular order of the fiber mode ($m_0 = \pm 1$ for a single-mode fiber) and χ is the relative amplitude of TE_z and TM_z waves that compose the total fiber mode. The latter is determined through the standard analysis of propagation in a straight and infinitely long optical fiber which can be found in any textbook on optical fibers. We quote its expression

$$\chi = \frac{k_f (a_f a_0 \alpha)^2}{(k_f^2 - k_0^2) m_0 \beta} \left[\frac{H'^{(2)}_{m_0}(a_0\alpha)}{a_0 \alpha H^{(2)}_{m_0}(a_0\alpha)} - \frac{J'_{m_0}(a_f\alpha)}{a_f \alpha J_{m_0}(a_f\alpha)}\right] \qquad (14)$$

where $a_0 = \sqrt{k_0^2 - \beta^2} = -j\sqrt{\beta^2 - k_0^2}$, $a_f = \sqrt{k_f^2 - \beta^2}$ and the prime denotes the derivative with respect to the argument. It is also reminded that, as in (12), (13) implies $z'_h = 0$. It is an interesting exercise to prove that, if the mode (13) is introduced into (1) and integrated along an infinitely long and straight fiber, the exterior field is exactly that derived through the standard analysis of propagation.

Returning to the field integral and by substituting (12) and (13) into (11), the integration over the angular variable φ'_h is done easily by virtue of the orthogonality property

$$\int_0^{2\pi} e^{j(m_0-n)\varphi'_h} d\varphi'_h = 2\pi\delta_{n,m_0} \tag{15}$$

where δ is Kronecker's delta (nonzero and equal to one only for $n = m_0$). Equation (11) then becomes

$$\begin{aligned} d\mathbf{E}(\mathbf{r}_h) \;=\; & -\frac{j}{4}(k_f^2 - k_0^2) dS e^{-j\beta S} \\ & \times \int_{-\infty}^{+\infty} dk \frac{(-1)^{m_0}}{a_0^2(k)} \left[\mathbf{M}^{(2)}_{m_0,k}(\mathbf{r}_h, k_0) \quad \mathbf{N}^{(2)}_{m_0,k}(\mathbf{r}_h, k_0)\right] \\ & \mathbf{A}_{m_0}(k,\beta) \begin{bmatrix} 1 \\ \chi \end{bmatrix} \end{aligned} \tag{16}$$

where $\mathbf{A}$ is the 2×2 matrix

$$\begin{aligned} \mathbf{A}_{m_0}(k,\beta) \;=\; & \begin{bmatrix} A_{11} & A_{12} \\ A_{21} & A_{22} \end{bmatrix} = \int_0^{\alpha} \begin{bmatrix} \mathbf{M}^{(1)}_{-m_0,-k}(\mathbf{r'}_h, k_0) \\ \mathbf{N}^{(1)}_{-m_0,-k}(\mathbf{r'}_h, k_0) \end{bmatrix} \\ & \bullet \left[\mathbf{M}^{(1)}_{m_0,-\beta}(\mathbf{r'}_h, k_1) \quad \mathbf{N}^{(1)}_{m_0,-\beta}(\mathbf{r'}_h, k_1)\right] \rho'_h d\rho'_h \end{aligned} \tag{17}$$

with $(\bullet)$ implying the inner product between the elements, i.e., vector waves $\mathbf{M}$, $\mathbf{N}$, of the generalized matrices, and of course $z'_h = 0$. After some lengthy algebra, the analytic expressions of the elements A_{ij} of matrix $\mathbf{A}$ are obtained

$$A_{11} = (-1)^{m_0} \frac{a_0 a_f \alpha}{k_0^2 - k_f^2} \left[a_0 J_{m_0}(a_0\alpha) J'_{m_0}(a_f\alpha) - a_f J'_{m_0}(a_0\alpha) J_{m_0}(a_f\alpha)\right]$$

$$A_{12} \;=\; (-1)^{m_0} \frac{m_0(-\beta)}{k_f} J_{m_0}(a_0\alpha) J_{m_0}(a_f\alpha)$$

$$
\begin{aligned}
A_{21}&=(-1)^{m_0}\frac{m_0 k}{k_0}J_{m_0}(a_0\alpha)J_{m_0}(a_f\alpha)\\
A_{22}&=(-1)^{m_0}\frac{a_0 a_f\alpha}{k_0 k_f(k_0^2-k_f^2)}\left[a_0 k_f^2 J_{m_0}(a_0\alpha)J'_{m_0}(a_f\alpha)\right.\\
&\quad\left.-a_f k_0^2 J'_{m_0}(a_0\alpha)J_{m_0}(a_f\alpha)\right]
\end{aligned}
\tag{18}
$$

where $a_0=(k_0^2-k^2)^{1/2}$, $a_f=(k_f^2-k^2)^{1/2}$ and a_0 obeys the sign selection stated in (9).

Equation (16) expresses the field contribution $d\mathbf{E}$ from the infinitesimal volume dV' of the fiber in terms of traveling cylindrical vector waves in the system (x_h, y_h, z_h). The orientation of the infinitesimal volume in space is shown in Fig. 5(b). To translate this field in terms of waves in the system (x_a, y_a, z_a), the transformation (7) is used. In the case of field computation in the interior of the helix ($\rho_0 < R$), this is written

$$
\begin{aligned}
\begin{pmatrix}\mathbf{M}^{(2)}_{m_0,k}(\mathbf{r}_h,k_0)\\ \mathbf{N}^{(2)}_{m_0,k}(\mathbf{r}_h,k_0)\end{pmatrix} &= \int_{-\infty}^{+\infty} dk_a \sum_{\nu=-\infty}^{+\infty}\mathbf{T}^{-\gamma,R}(\nu,k_a,m_0,k)\\
&\quad\cdot\begin{pmatrix}\mathbf{M}^{(1)}_{\nu,k_a}(\mathbf{r}_a,k_0)\\ \mathbf{N}^{(1)}_{\nu,k_a}(\mathbf{r}_a,k_0)\end{pmatrix}
\end{aligned}
\tag{19}
$$

where k_a is the wave number along the z_a-direction, i.e., the axis of the helix, R is the helix radius, measured from the axis of the helix to the axis of the fiber and the selection of angle $-\gamma$ as the rotation angle is immediately justified by an inspection of Figs. 3 and 4.

System (x_a, y_a, z_a) is an elevated and rotated around the axis of the helix version of the fixed system (x_0, y_0, z_0). Therefore, to further translate the field in terms of waves in (x_0, y_0, z_0) we combine the transformations (4) and (5) to obtain

$$
\begin{pmatrix}\mathbf{M}^{(1)}_{\nu,k_a}(\mathbf{r}_a,k_0)\\ \mathbf{N}^{(1)}_{\nu,k_a}(\mathbf{r}_a,k_0)\end{pmatrix}=\begin{pmatrix}\mathbf{M}^{(1)}_{\nu,k_a}(\mathbf{r}_0,k_0)\\ \mathbf{N}^{(1)}_{\nu,k_a}(\mathbf{r}_0,k_0)\end{pmatrix}e^{-j(\nu\varphi+k_a h)}
\tag{20}
$$

where φ, h are, respectively, the polar rotation and elevation of the current point of the helix, i.e., the point that corresponds to the current length S where the volume dV' is located. From the properties of the helix examined in Section 2.2, we have the obvious relationships $\varphi = S\sin\gamma/R = 2\pi S\cos\gamma/P$ and $h=\varphi P/(2\pi)=S\cos\gamma$. After (19)

and (20), (16) is rewritten

$$d\mathbf{E}(\mathbf{r}_0) = (k_f^2 - k_0^2) dS e^{-j\left(\beta + \frac{2\pi\nu}{P}\cos\gamma\right)S} \left(-\frac{j}{4}\right) \int_{-\infty}^{+\infty} dk \frac{(-1)^{m_0}}{a_0^2(k)} \int_{-\infty}^{+\infty} dk_a e^{-jk_a S\cos\gamma} \times \sum_{\nu} \left[\mathbf{M}^{(1)}_{\nu,k_a}(\mathbf{r}_0, k_0) \quad \mathbf{N}^{(1)}_{\nu,k_a}(\mathbf{r}_0, k_0)\right] \mathbf{T}^{-\gamma,R}(\nu, k_a, m_0, k)\mathbf{A}_{m_0}(k,\beta) \begin{bmatrix} 1 \\ \chi \end{bmatrix} \tag{21}$$

which is a desired expression in terms of standing vector waves (Bessel function radial dependence) in the fixed system (x_0, y_0, z_0).

In order to compute the total field induced at the point $\mathbf{r}_0$ the contributions $d\mathbf{E}$ must be integrated as the current point runs along the fiber, i.e.,

$$\mathbf{E}(\mathbf{r}_0) = \int_{S=-\infty}^{+\infty} d\mathbf{E}(\mathbf{r}_0) \tag{22}$$

From (21), it is apparent that the integration over S yields a Dirac function factor:

$$\int_{-\infty}^{+\infty} e^{-j\left(\beta + \frac{2\pi\nu}{P}\cos\gamma + k_a\cos\gamma\right)S} dS = \frac{2\pi}{\cos\gamma}\delta\left(k_a + \frac{\beta}{\cos\gamma} + \frac{2\pi\nu}{P}\right) \tag{23}$$

The presence of the Dirac function inside (21) eliminates the integration over k_a and keeps only the wave number $k_a = -(\beta/\cos\gamma + 2\pi\nu/P)$. The final result is

$$\mathbf{E}(\mathbf{r}_0) = (k_f^2 - k_0^2)\left(-\frac{\pi j}{2\cos\gamma}\right) \times \sum_{\nu=-\infty}^{+\infty} \left[\mathbf{M}^{(1)}_{\nu,k_\nu}(\mathbf{r}_0, k_0) \quad \mathbf{N}^{(1)}_{\nu,k_\nu}(\mathbf{r}_0, k_0)\right] \cdot \mathbf{C}_\nu(m_0,\beta) \cdot \begin{bmatrix} 1 \\ \chi \end{bmatrix} \tag{24}$$

where $k_\nu = -\beta/\cos\gamma - 2\pi\nu/P$ and $\mathbf{C}$ is a 2×2 matrix of complex coefficients and is given by

$$\mathbf{C}_\nu(m_0,\beta) = \int_{-\infty}^{+\infty} dk \frac{(-1)^{m_0}}{a_0^2(k)} \mathbf{T}^{-\gamma,R}(\nu, k_\nu, m_0, k)\mathbf{A}_{m_0}(k,\beta) \tag{25}$$

Equation (24) is the final analytical expression of the electric field inside the cylinder defined by the helix ($\rho_0 < R$). The magnetic field is obtained by taking the curl of (24) and dividing with $-j\omega\mu_0$. By virtue of the mirror property $\nabla \times \mathbf{M} = k_0\mathbf{N}$ and $\nabla \times \mathbf{N} = k_0\mathbf{M}$, this is equivalent to simply interchanging the $\mathbf{M}$ and $\mathbf{N}$ waves and multiplying by jY_0 where Y_0 is the wave admittance of free-space ($Y_0 = \sqrt{\varepsilon_0/\mu_0}$). Note also how the elements C_{ij} of matrix $\mathbf{C}$ are combined to yield the amplitude of the TE_z and TM_z waves that constitute the total field: The amplitudes of the $\mathbf{M}$ and $\mathbf{N}$ waves are respectively proportional to $C_{11} + \chi C_{12}$ and $C_{21} + \chi C_{22}$, for the electric field, and vice-versa for the magnetic field.

It is important to recognize the effect of the geometrical evolution of the helical path in space on the expression of the produced field. From (24), it is straightforward to prove that the components of the electric (and magnetic) field in the fixed cylindrical coordinates (ρ_0, φ_0, z_0) satisfy

$$\Psi\left(\rho_0, \varphi_0 + \frac{2\pi h}{P}, z_0 + h\right) = \Psi\left(\rho_0, \varphi_0, z_0\right) e^{-j\beta\left(\frac{h}{\cos\gamma}\right)} \tag{26}$$

where Ψ can be any component ρ, φ or z of field $\mathbf{E}$ or $\mathbf{H}$. This is clearly a result of the helical geometry of the fiber, stating that the field amplitude is invariant under a helical transformation of the coordinate system (i.e., an arbitrary z-elevation by h and a subsequent φ-rotation by $2\pi h/P$) and the phase is increased by $\beta h/\cos\gamma$ which is exactly the phase acquired by the fiber mode propagating with constant β over the corresponding length of the helix for elevation h, namely $h/\cos\gamma$. Property (26) can be thought as a mixed axial-angular quasi-periodicity condition. Also, in complete analogy to the Hartree space harmonics that compose the quasi-periodic Bloch modes in periodic structures, (24) can be viewed as the representation of the field in terms of mixed axial-angular Hartree special harmonics with z-propagation constants that differ by integer multiples of $2\pi/P$. Due to the simultaneous periodicity of a helical structure in the z and φ coordinates, the order of the Hartree harmonic (ν) is here the angular order in the φ coordinate, i.e., the harmonics have a mixed dependence $\exp[j\nu(\varphi - 2\pi z/P)]$. From the latter it is clear that if an observer follows a helical path with constant $\varphi - 2\pi z/P$ and arbitrary radius, then the observed field will be invariant except from the mentioned phase factor. This is of course expected because, since the helix is of infinite length, the above observer sees always the same structure. If a complete 2π-arc is completed in the φ coordinate, then (26) reduces to the Bloch condition of the field due to the P-periodicity in the z-

direction. Explicitly by setting $h = P$ in (26) we obtain

$$\Psi(\rho_0, \varphi_0, z_0 + h) = \Psi(\rho_0, \varphi_0, z_0)\, e^{-j\beta L} \tag{27}$$

where $L = P/\cos\gamma$ is the length of a helix turn.

Equation (24) gives the filed in the interior of the helix, i.e., for $\rho_0 < R$. In this region the transformation of vector waves between the coordinate systems (x_h, y_h, z_h) and (x_a, y_a, z_a) has a uniform expression as the current origin point $x_h = y_h = z_h = 0$, which is enclosed in the elementary volume dV', runs along the helix. From a careful study of the procedure detailed in [1], it is obvious that this is because all points in the region $\rho_0 < R$ have positive variable y_h, i.e., $y_h > 0$. This consequently means that the waves needed to express vector waves in the new skew system (x_a, y_a, z_a) decay and/or propagate to the positive y_h-direction, which is evident from the presence of phase factor $\exp(jk'_y d)$ in (7), reminding that $\mathrm{Re}(k'_y) < 0$, $\mathrm{Im}(k'_y) > 0$ from (9).

However, the computation of the field in the exterior of the helix ($\rho_0 > R$) is more complicated. For a point of observation with $\rho_0 > R$, there is a part of each helix turn that "sees" that point with $y_h < 0$, resulting in a different expression of the transformation matrix applying for the waves emanating from these helix parts. It is easy to find that all these parts are projected onto a $2\xi_0$-arc, of the circle $\rho_0 = R$ on the polar plane $z_0 = 0$, with $\xi_0 = \cos^{-1}(R/\rho_0)$, as shown in Fig. 6. For these parts, the transformation is given by an expression identical to (19) but with a matrix $\tilde{\mathbf{T}}$ which is given by replacing factor

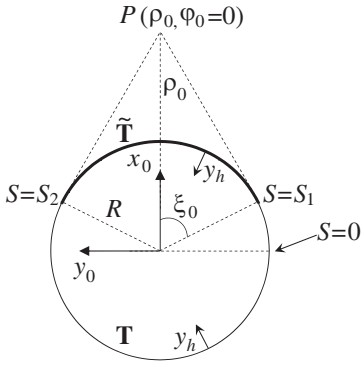

Figure 6. Top view of the helix showing the part (solid arc) for which transformation matrix $\tilde{\mathbf{T}}$ applies (points with $y_h < 0$). The points of the characteristic helix lengths S_1, S_2 that define these parts are also shown. An observation point with $\rho_0 > R$ and $\varphi_0 = 0$ has been assumed.

$\exp(jk'_y d)$ with $\exp(-jk'_y d)$, variable τ with $\pi - \tau$ and variable w with $-w$ in expressions (8).

In order to perform the integration of (1) we assume an observation point with polar coordinates (ρ_0, φ_0) and $\rho_0 > R$. Since we have assumed $S = 0$ at a point of the helix with $\varphi_0 = -\pi/2$ (see Fig. 6 and also note that the z_0-coordinate of that point can also be arbitrarily set $z_0 = 0$), the parts of the helix, along which the transformation matrix $\tilde{\mathbf{T}}$ must be used, are included between the characteristic helix lengths

$$\begin{aligned} S_1(\varphi_0, n) &= \left(2n\pi + \varphi_0 + \frac{\pi}{2} - \xi_0\right) \frac{R}{\sin\gamma} \\ S_2(\varphi_0, n) &= \left(2n\pi + \varphi_0 + \frac{\pi}{2} + \xi_0\right) \frac{R}{\sin\gamma} \end{aligned} \tag{28}$$

where n takes all integer values $(n =, \ldots, -1, 0, 1, \ldots,)$ and $\xi_0 = \cos^{-1}(R/\rho_0)$. Note that the offset of $\pi/2$ is due to the fact that the fixed system "sees" the $S = 0$ point with polar angle $\varphi_0 = -\pi/2$ (see Fig. 6). Because the transformation matrix $\tilde{\mathbf{T}}$ is used over the parts of the helix between lengths $S_1(\varphi_0, n)$ and $S_2(\varphi_0, n)$and matrix $\mathbf{T}$ over the rest parts, the following series need to be computed

$$\begin{aligned} I_{\tilde{\mathbf{T}}}(K, \varphi_0) &= \sum_{n=-\infty}^{+\infty} \left(\int_{S_1(\varphi_0, n)}^{S_2(\varphi_0, n)} e^{-jKS} dS \right) \\ I_{\mathbf{T}}(K, \varphi_0) &= \sum_{n=-\infty}^{+\infty} \left(\int_{S_2(\varphi_0, n)}^{S_1(\varphi_0, n) + 2\pi R/\sin\gamma} e^{-jKS} dS \right) \end{aligned} \tag{29}$$

where for brevity we have set $K = \beta + k_a \cos\gamma + 2\pi\nu P^{-1} \cos\gamma$. After completing the necessary algebra, it can be shown that

$$\begin{aligned} I_{\tilde{\mathbf{T}}}(K, \varphi_0) &= 2\xi_0 \sum_{m=-\infty}^{+\infty} \text{sin c}\left(\frac{\xi_0 m}{\pi}\right) e^{-jm(\varphi_0 + \pi/2)} \delta\left(K - \frac{2\pi m}{L}\right) \\ I_{\mathbf{T}}(K, \varphi_0) &= 2\pi\delta(\text{K}) - I_{\tilde{\mathbf{T}}}(K, \varphi_0) \end{aligned} \tag{30}$$

where $\text{sin c}(x) \equiv \sin(\pi x)/(\pi x)$ is the sampling function and δ is Dirac's function. To obtain (30), we have used the familiar Fourier series identity of the Dirac comb

$$\frac{2\pi}{L} \sum_{m=-\infty}^{+\infty} \delta\left(K - \frac{2\pi m}{L}\right) = \sum_{m=-\infty}^{+\infty} e^{jmKL} \tag{31}$$

Therefore, when $d\mathbf{E}(\mathbf{r}_0)$ is integrated in Eq. (22) and Eqs. (30) are used, we find that the result contains the factor

$$\tilde{\mathbf{T}} \cdot I_{\tilde{\mathbf{T}}}(K) + \mathbf{T} \cdot I_{\mathbf{T}}(K) = \Big[\mathbf{T} \cdot 2\pi\delta(K) + (\tilde{\mathbf{T}} - \mathbf{T}) \cdot 2\xi_0 \sum_{m=-\infty}^{+\infty} \text{sin c}\left(\frac{\xi_0 m}{\pi}\right) e^{-jm(\varphi_0+\pi/2)} \delta\left(K - \frac{2\pi m}{L}\right)\Big] \tag{32}$$

which must be integrated over all real wave numbers k_a. Then the first term of (32) yields apparently an expression identical to (24), while the second yields a complicated double series term, over the wave numbers $k_a \equiv k_{\nu m}$ that satisfy $K = 2\pi m/L$. In conclusion, the final result for the field for $\rho_0 > R$ is written as the sum of two field terms

$$\mathbf{E}(\mathbf{r}_0) = \mathbf{E}_1(\mathbf{r}_0) + \mathbf{E}_2(\mathbf{r}_0) \tag{33}$$

where

$$\mathbf{E}_1(\mathbf{r}_0) = (k_f^2 - k_0^2)\left(-\frac{\pi j}{2\cos\gamma}\right) \times \sum_{\nu=-\infty}^{+\infty} \left[\mathbf{M}^{(1)}_{\nu,k_\nu}(\mathbf{r}_0, k_0) \quad \mathbf{N}^{(1)}_{\nu,k_\nu}(\mathbf{r}_0, k_0)\right] \cdot \mathbf{C}_\nu(m_0, \beta) \cdot \begin{bmatrix} 1 \\ \chi \end{bmatrix} \tag{34}$$

with matrix $\mathbf{C}$ previously defined in (25) and

$$\mathbf{E}_2(\mathbf{r}_0) = (k_f^2 - k_0^2)\left(\frac{-\pi j}{2\cos\gamma}\right)\left(\frac{\xi_0}{\pi}\right) \int_{-\infty}^{+\infty} dk \frac{(-1)^{m_0}}{a_0^2(k)} \left\{ \sum_{m=-\infty}^{+\infty} \sum_{\nu=-\infty}^{+\infty} \text{sin c}\left(\frac{\xi_0 m}{\pi}\right) \exp\left[-jm\left(\frac{\pi}{2} + \varphi_0\right)\right] \mathbf{W}^{(1)}_{\nu,k_{\nu m}}(\mathbf{r}_0, k_0) \cdot (\tilde{\mathbf{T}} - \mathbf{T})^{-\gamma,R}(\nu, k_{\nu m}, m_0, k) \right\} \mathbf{A}_{m_0}(k, \beta) \cdot \begin{bmatrix} 1 \\ \chi \end{bmatrix} \tag{35}$$

where the axial wave numbers take the discrete values $k_{\nu m} = -\beta/\cos\gamma + 2\pi(m-\nu)/P$ and, for brevity, the $\mathbf{M}$, $\mathbf{N}$ waves have been included in a generalized 1×2 vector $\mathbf{W} = [\mathbf{M} \quad \mathbf{N}]$.

It is straightforward to verify that the field in the region $\rho_0 > R$ satisfies the same quasi-periodic conditions (26) and (27) with the field in the region $\rho_0 < R$. Note that as $\rho_0 \to R^+$ the angle $\xi_0 \to 0$ which consequently means that $\mathbf{E}_2(\mathbf{r}_0) \to 0$ and $\mathbf{E}(\mathbf{r}_0) \to \mathbf{E}_1(\mathbf{r}_0)$, which is equal to the limit of the field from the inner side, i.e., for $\rho_0 \to R^-$ due to the same expressions (24) and (34).

3. CONCLUSION

We have reported a completely analytical computation of the electromagnetic field produced by an optical fiber helix. The approach utilized the transformation of radially traveling cylindrical waves between two skew cylindrical coordinates systems that has been previously derived by the author, and has so far been used only in the context of coupling between two non-parallel optical fibers. A set of realistic assumptions were invoked in order to validate the applicability of the analysis and discard phenomena of cross-polarization coupling inside the fiber, bend loss and interaction between the helix turns, so that the guided fiber mode can be adiabatically translated along the helical path. We obtained elegant analytical formulas for the field inside and outside of the cylinder defined by the helix in terms of mixed axial- and angular- space harmonics and established the simultaneous angular-axial quasi-periodic conditions satisfied by the electromagnetic field due to the helical geometry of the optical path. An interesting two-term decomposition of the outward radiated field was reached, which resulted from a periodic segmentation of the helix length due to the different transforming expressions over different parts of the helix. In a future work we will address the non-trivial issue of applying the derived expressions numerically and study the resulting field distributions.

REFERENCES

1. Chremmos, I. D. and N. K. Uzunoglu, "Transformation of radially traveling cylindrical waves between two skew cylindrical coordinate systems," *J. Opt. Soc. Am. A*, Vol. 23, 1884–1888, 2006.
2. Abramowitz M. and I. A. Stegun, *Handbook of Mathematical Functions*, Dover, New York, 1972.
3. Chremmos, I. D., N. K. Uzunoglu, and G. Kakarantzas, "Rigorous analysis of the coupling between two nonparallel optical fibers," *IEEE J. Lightwave Technol.*, Vol. 24, 3779–3788, 2006.
4. Tong, L. M., R. R. Gattass, J. B. Ashcom, S. L. He, J. Y. Lou, M. Y. Shen, I. Maxwell, and E. Mazur, "Subwavelength-diameter silica wires for low-loss optical wave guiding," *Nature*, Vol. 426, 816–819, 2003.
5. Sumetsky, M., "Basic elements for microfiber photonics: Micro/nanofibers and microfiber coil resonators," *J. Lightwave Technology*, Vol. 26, 21–27, 2008.

6. Xu, F. and G. Brambilla, "Manufacture of 3-D microfiber coil resonators," *IEEE Photon. Technol. Lett.*, Vol. 19, 1481–1483, 2007.
7. Sumetsky, M., "Optical fiber microcoil resonator," *Opt. Express*, Vol. 12, 2303–2316, 2004.
8. Tai, C. T., *Dyadic Green Functions in Electromagnetic Theory*, IEEE Press, 1994.
9. Collin, R. E., *Field Theory of Guided Waves*, McGraw-Hill, New York, 1960.